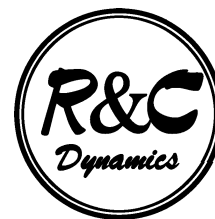


P. E. RYABOV

Department of Mathematical Modelling
Moscow State Technical University after N. E. Bauman
2-nd Baumanskaya, 5, Moscow, 107005, Russia
E-mail: orelryabov@mtu-net.ru



BIFURCATION SETS IN AN INTEGRABLE PROBLEM ON MOTION OF A RIGID BODY IN FLUID

Received November 20, 1999

In the paper we obtain the bifurcation sets for a family of Liouville integrable Hamiltonian systems with the additional integral of fourth degree.

To the 150th Anniversary of S. V. Kovalevskaya

1. Introduction

Among classical papers, concerning integration of equations of motion of a rigid body about a fixed point and motion of a body in fluid, we would like to quote two ones with the additional integrals of fourth degree: the papers by Kovalevskaya [23] and by Chaplygin [7]. It is known that the general solution of the system of six Euler–Poisson equations in the Kovalevskaya case is very complicated, it is expressed in terms of ultraelliptic functions. Therefore, degenerate cases of this solution, when the ultraelliptic integrals become elliptic, are of particular interest. Degeneration of quadratures results in the fact that some polynomial related to separation of variables (in the Kovalevskaya case it is the polynomial of fifth degree) has multiple roots for some values of integrals. Particular motions, corresponding to these values of the first integrals, were first found by Appelrot [1]. More detailed analysis of these motions was carried out by Ipatov [14]. It turned out [18] that they are precisely Appelrot classes that correspond to the cases of *dependence between first integrals*. If we know the conditions, under which the first integrals are dependent, in other words, *the bifurcation set*, we can profitably study degenerate cases *without* separation of variables, since each class of degenerate motions has its intrinsic properties. For the Kovalevskaya case this method was successfully realized by Dokshevich [8, 9, 10, 11]. Finally, using Morse-type theory for integrable Hamiltonian systems obtained by Bolsinov and Fomenko [4] it is possible to clarify the behavior of the system *as a whole* in terms of some invariants. This theory also enables us to describe change of qualitative behavior of integral trajectories during bifurcations of so-called Liouville tori. The complete classification of Kovalevskaya-type dynamical systems up to Liouville equivalence was given by Bolsinov, Fomenko and Richter [5].

Thus, the condition of multiplicity of roots of some polynomials allows us to write down explicit equations for bifurcation curves and then to integrate the system along the bifurcation curves. This explicit integration helps us to give a description of local behavior of the system near the bifurcation set, and thereafter of global behavior of the system. This approach can be used even in integrable problems, for which separation of variables is not found.

In the original paper [7] Chaplygin considered a problem that describes a particular case of motion of a rigid body in a perfect incompressible fluid. The fluid is unbounded in all directions and is at rest at infinity; the body is bounded by a simply-connected surface. We assume that the body and the fluid are under the gravitation force, we also assume that the weight of the body is equal to the weight

Mathematics Subject Classification 35Q05

of the fluid displaced. In terms of dimensionless variables this motion is described by the following system of the Kirchhoff equations:

$$\begin{aligned} \dot{s}_1 &= -s_3 s_2 - cr_2 r_3 + \delta r_3, & \dot{r}_1 &= s_2 r_3 - 2s_3 r_2, \\ \dot{s}_2 &= s_3 s_1 - cr_1 r_3 - \gamma r_3, & \dot{r}_2 &= 2s_3 r_1 - s_1 r_3, \\ \dot{s}_3 &= 2cr_1 r_2 + \gamma r_2 - \delta r_1, & \dot{r}_3 &= s_1 r_2 - s_2 r_1, \end{aligned} \quad (1.1)$$

where c, δ, γ are some constants. Here the vectors \vec{s}, \vec{r} are called the momentum and the momentum force.

The first integrals of these equations have the form

$$\begin{aligned} f_1 &= r_1^2 + r_2^2 + r_3^2 = f, & (\text{geometric integral}) \\ f_2 &= s_1 r_1 + s_2 r_2 + s_3 r_3 = g, & (\text{area integral}) \\ H &= \frac{1}{2}(s_1^2 + s_2^2 + 2s_3^2) + \frac{1}{2}(c(r_1^2 - r_2^2) + 2\gamma r_1 + 2\delta r_2) = h. & (\text{Hamiltonian}) \end{aligned}$$

Chaplygin [7] showed that if the area integral is equal to zero, then the system (1.1) has the additional integral

$$F = (s_1^2 - s_2^2 + cr_3^2 - 2\gamma r_1 + 2\delta r_2)^2 + 4(s_1 s_2 - \gamma r_2 - \delta r_1)^2 = k.$$

If $c = 0$, then the area integral is not necessarily zero, and we come to the problem on motion of a rigid body about a fixed point in the Kovalevskaya case. Bifurcations of the first integrals in this problem were studied by Kharlamov [18].

The papers by Kharlamov [15, 16, 17], by Rubanovsky [26], and by Yehia [28] are devoted to integrable cases of motion of a rigid body bounded by a multiply-connected surface in fluid. Under the conditions as before this motion can be described in terms of dimensionless variables by the following Kirchhoff-type system of equations:

$$\begin{aligned} \dot{s}_1 &= -(s_3 - \lambda)s_2 - cr_2 r_3 + \delta r_3, & \dot{r}_1 &= s_2 r_3 - 2s_3 r_2, \\ \dot{s}_2 &= (s_3 - \lambda)s_1 - cr_1 r_3 - \gamma r_3, & \dot{r}_2 &= 2s_3 r_1 - s_1 r_3, \\ \dot{s}_3 &= 2cr_1 r_2 + \gamma r_2 - \delta r_1, & \dot{r}_3 &= s_1 r_2 - s_2 r_1. \end{aligned} \quad (1.2)$$

The parameter of the gyrostatic momentum λ can be related to the circulation of the fluid through the holes inside the body. As before, the vectors \vec{s}, \vec{r} are called the momentum and the momentum force.

The first integrals of these equations have the form

$$\begin{aligned} f_1 &= r_1^2 + r_2^2 + r_3^2 = f, & (\text{geometric integral}) \\ f_2 &= s_1 r_1 + s_2 r_2 + (s_3 + \lambda)r_3 = 0, & (\text{area integral}) \\ H &= \frac{1}{2}(s_1^2 + s_2^2 + 2s_3^2) + \frac{1}{2}(c(r_1^2 - r_2^2) + 2\gamma r_1 + 2\delta r_2) = h, & (\text{Hamiltonian}) \\ F &= (s_1^2 - s_2^2 + cr_3^2 - 2\gamma r_1 + 2\delta r_2)^2 + 4(s_1 s_2 - \gamma r_2 - \delta r_1)^2 + \\ &\quad + 8\lambda(s_3 - \lambda)(s_1^2 + s_2^2) - 8\lambda r_3 \{s_1(2\gamma + cr_1) + s_2(2\delta - cr_2)\} = k. & (\text{additional integral}) \end{aligned}$$

Note that the additional integral F was also found by Yehia [28].

If $c = 0$, then the area integral is not necessarily zero, and we come to the problem on motion of a heavy gyrost at under the Kovalevskaya conditions imposed on the distribution of mass. The papers [13] and [20] are devoted to the topological analysis of this problem.

Notice that with the help of some linear changes of variables, time, and parameters, we can make the value f of the geometric integral and the constant c equal to 1. These changes do not influence on the topological analysis of the problem, and in what follows we take $f = 1, c = 1$.

The systems (1.1) and (1.2) are Hamiltonian on the orbit $M^4 = \{f_1 = 1, f_2 = 0\}$. The additional integrals are almost everywhere independent with the Hamiltonians, therefore, the systems are complete integrable by Liouville. According to the Liouville–Arnold theorem [2], the nonsingular compact common level of the first integrals is a union of tori filled with quasi-periodic trajectories. After going through the singular levels of the first integrals, these tori bifurcate in some manner.

In the paper we study topology of energy surfaces $Q_h^3 = \{H = 2h\}$ and obtain the bifurcation sets, we also describe bifurcations of Liouville tori in the Chaplygin problem and its generalization. For some values of the parameters we calculate the Fomenko invariant and partially the Fomenko–Zieschang invariant.

The author expresses his deep gratitude to O. E. Orel for useful advices and discussions.

2. Necessary definitions

The *momentum mapping* is a mapping $\Phi: M^4 \rightarrow \mathbb{R}^2$ that assigns to a point on the manifold the pair of values of the functions H and F at this point: $x \rightarrow (H(x), F(x))$. Obviously, a Liouville torus is mapped into a single point. The *set of singularities* of the momentum mapping is the set of points of M^4 , at which the functions H and F are dependent: $K = \{x \in M^4: \text{rank } d\Phi(x) < 2\}$. The image $\Sigma = \Phi(K)$ of this set is called the *bifurcation set*. By $Q_h^3 = \{x \in M^4 | H(x) = h\}$ we denote the *energy surface*. In what follows we assume that this surface is nonsingular and compact.

In [12] Fomenko obtained the Morse-type theory for integrable Hamiltonian systems. In the framework of this theory global behavior of a system on an energy surface can be described with the help of some graph. The edges of the graph (=molecule) correspond to one-parameter families of nonsingular Liouville tori, and its vertices (=atoms) describe bifurcations of these tori on singular levels of the integral F . This graph is denoted by $W(Q_h^3)$ and called the *Fomenko invariant*. Besides, if we complete the molecule W with some numerical marks r_i, ε_i, n_k , we obtain the *Fomenko–Zieschang invariant*, or the *marked molecule*, which is denoted by W^* . In particular, the numerical marks r_i describe the rules of gluing of Liouville tori on the edges of the molecule.

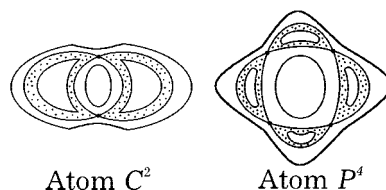


Fig. 1

The simplest bifurcations (atoms) are denoted by the characters A, B, A^* : the bifurcation A characterizes degeneration of a torus into a circle, B denotes splitting of a torus into two ones (or, conversely, gluing of two tori), and A^* — the complicated bifurcation of a torus to another torus. Besides, in integrable problems with some symmetries one can meet atoms C_2 and P_4 . The first of them describes a symmetric bifurcation of two tori to two tori, and the second — a symmetric bifurcation of two tori to four tori. The atoms C_2 and P_4 are illustrated in Fig. 1.

In what follows we use a notation $\Sigma(\lambda)$ for the bifurcation set; therefore, $\Sigma(0)$ is a bifurcation set for the classical Chaplygin problem [7].

Further notions and definitions are related to stationary points of the systems (1.1) and (1.2). The *rank* of a point $x \in M^4$ is the rank of the momentum mapping $\text{rank } d\Phi(x)$ at this point. Let $x \in M^4$ be a point of zero rank, and suppose $\Phi(x) = (k, h)$. Let U be a small regular neighborhood of the point (k, h) such that its boundary ∂U intersects the bifurcation diagram transversely at minimal number of points. The loop molecule $W(\Phi^{-1}(\partial U))$ completely describes topology of Liouville foliation in the neighborhood of the point of zero rank. The *zero-rank multiplicity* of the point (k, h) is a number of points of zero rank in the preimage $\Phi^{-1}(k, h)$. In the paper [6] all saddle-saddle singularities of zero-rank multiplicity two are classified with the help of the l -type introduced in [3]. The results are represented in the form of the list of loop molecules. One of this molecule that contains atoms C_2 and P_4 is illustrated in Fig. 2. We will meet this molecule in what follows.

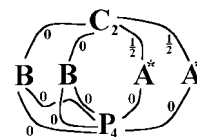


Fig. 2. Loop molecule with the atoms C_2 and P_4

3. Topology of Q_h^3

We describe the topology of Q_h^3 according to the values of the parameters (δ, γ) in the case, when the parameter λ is zero. Figure 3 demonstrates the domains of the same topological type of Q_h^3 : a) if $\delta = \gamma = 0$, then it is equal to \emptyset for $h < -\frac{1}{2}$, to $2S^3$ for $-\frac{1}{2} < h < 0$, $S^1 \times S^2$ for $0 < h < \frac{1}{2}$, to $\mathbb{R}P^3$ for $\frac{1}{2} < h$; b) if $\delta = 0$ or $\gamma = 0$, then it is equal to S^3 , $2S^3$, $S^1 \times S^2$, $\mathbb{R}P^3$ (in the case $\gamma = 0$ the separating curves are marked off by bold lines in Fig. 5); c) if $(\delta, \gamma) \in A$, then it is equal to S^3 , $\mathbb{R}P^3$; d) if $(\delta, \gamma) \in B \cup C$, then it is equal to S^3 , $2S^3$, $\mathbb{R}P^3$; e) if $(\delta, \gamma) \in D$, then it is equal to S^3 , $2S^3$, $S^1 \times S^2$, $\mathbb{R}P^3$. Note that the surface Q_h^3 is never diffeomorphic to the connected sum $(S^1 \times S^2) \# (S^1 \times S^2)$, which is typical for the Kovalevskaya case. Probably, the reason is that our problem is integrable only at zero area integral. However, the gyrostatic momentum λ gives rise to the manifold $N^3 = (S^1 \times S^2) \# (S^1 \times S^2) \# (S^1 \times S^2)$, as is shown in the following theorem.

Theorem 1. *If $\lambda \neq 0$ and $\delta = \gamma = 0$, then the energy surface Q_h^3 has the following topological type: $2S^3$, $S^1 \times S^2$, $N^3 = (S^1 \times S^2) \# (S^1 \times S^2) \# (S^1 \times S^2)$, and $\mathbb{R}P^3$. The topological types of Q_h^3 and the separating curves (marked off by bold lines) are illustrated in Fig. 6.*

Proof.

Topological type of the energy surface $Q_h^3 = \{H = h\}$ can be studied with the help of the projection π onto the Poisson sphere $S^2 = \{r_1^2 + r_2^2 + r_3^2 = 1\}$ (see [27, 19, 25]). In our case, this projection takes the surface Q_h^3 onto a domain on the Poisson sphere given by the condition

$$\varphi_\lambda(r) \leq h, \quad (3.1)$$

where

$$\varphi_\lambda(r) = \frac{1}{2}(r_1^2 - r_2^2) + \frac{\lambda^2 r_3^2}{2 - r_3^2}.$$

Here the surface Q_h^3 is stratified over this domain with the circle fiber contracted to a point over the boundary.

The function $\varphi_\lambda(r)$ is the Morse function on the sphere. The critical points and the values of the function at these points are the following:

1. $r_2 = r_3 = 0$, $r_1^2 = 1$, $\varphi_\lambda(r) = \frac{1}{2}$,
2. $r_1 = r_3 = 0$, $r_2^2 = 1$, $\varphi_\lambda(r) = -\frac{1}{2}$,
3. $r_2 = r_1 = 0$, $r_3^2 = 1$, $\varphi_\lambda(r) = \lambda^2$,
4. $r_2 = 0$, $r_1^2 = 1 - r_3^2$, $1 - \frac{4\lambda^2}{(2 - r_3^2)^2} = 0$, $\varphi_\lambda(r) = \frac{1}{2} - (1 - \lambda)^2$, $\lambda \in \left[\frac{1}{2}, 1\right]$,
 $\varphi_\lambda(r) = \frac{1}{2} - (1 + \lambda)^2$, $\lambda \in \left[-1, -\frac{1}{2}\right]$.

The lines $h = \pm\frac{1}{2}$ and the parabolas $h = \lambda^2$, $h = \frac{1}{2} - (1 - \lambda)^2$, $\lambda \in \left[\frac{1}{2}, 1\right]$, $h = \frac{1}{2} - (1 + \lambda)^2$, $\lambda \in \left[-1, -\frac{1}{2}\right]$, form the bifurcation diagram in the plane $\mathbb{R}^2(\lambda, h)$ (see Fig. 6). It is symmetric with respect to the line $\lambda = 0$. The points A and C have the following coordinates: $A\left(\frac{1}{2}, \frac{1}{4}\right)$, $C\left(1, \frac{1}{2}\right)$.

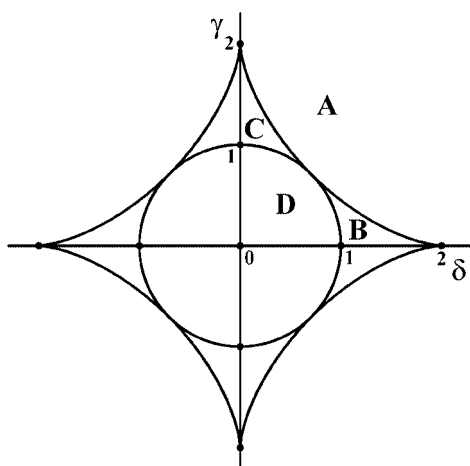


Fig. 3

On the line $h = -\frac{1}{2}$ the critical points have index 0. On the line $h = \frac{1}{2}$ they have index 2 between the points of contact of the line and the parabolas $h = \frac{1}{2} - (1 \pm \lambda)^2$, and index 1 otherwise. On the parabola $h = \lambda^2$ the index is equal to 1 between the points of contact of the parabola and the parabolas $h = \frac{1}{2} - (1 \pm \lambda)^2$, it is equal to 2 otherwise. Consider the segment AC of the parabola $h = \frac{1}{2} - (1 - \lambda)^2$, $\lambda \in \left(\frac{1}{2}, 1\right)$. Each point (λ_0, h_0) of the parabola corresponds to four critical points of index 1 with the coordinates (r_1^0, r_2^0, r_3^0) , where $r_2^0 = 0$, $(r_1^0)^2 = 1 - (r_3^0)^2$, $(r_3^0)^2 = 2 - 2\lambda_0$. We consider, for example, the point with $r_3^0 \in (0, 1)$. We take the pair (r_2, r_3) as local coordinates in the neighborhood of this point. We put $r_2 = x, r_3 = y - r_3^0$, where $(r_3^0)^2 = 2 - 2\lambda_0$. The expansion of the function φ_{λ_0} in the neighborhood of this point has the form

$$\varphi_{\lambda_0}(x, y) = \frac{1}{2} - \frac{1}{4}(r_3^0)^4 - \frac{1}{2}x^2 + \left(\frac{2(r_3^0)^2}{2 - (r_3^0)^2}\right)y^2 + o(x^2 + y^2).$$

Therefore, we come to the conclusion required. With the help of indices of the critical points we obtain the topological type of domains (3.1) on the Poisson sphere: they are \emptyset , two disks D^2 , the annulus $\mathbb{S}^1 \times \mathbb{R}^1$ (the disk D^2 with one hole), the disk D^2 with three holes, the sphere \mathbb{S}^2 . The corresponding surfaces Q_h^3 are homeomorphic to $2\mathbb{S}^3$, $\mathbb{S}^1 \times \mathbb{S}^2$, $N^3 = (\mathbb{S}^1 \times \mathbb{S}^2) \# (\mathbb{S}^1 \times \mathbb{S}^2) \# (\mathbb{S}^1 \times \mathbb{S}^2)$, and $\mathbb{R}P^3$. Theorem is proved. ■

4. Bifurcation set and bifurcations of Liouville tori

The bifurcation set Σ plays the fundamental role in the study of global behavior of integrable Hamiltonian systems. Here we give a review of the results concerned with the bifurcation set in the case, when the parameter of the gyrostatic moment λ is equal to zero (the relevant proofs will be published in a separate paper).

Theorem 2. *The bifurcation set $\Sigma(0)$ is*

a) *the union of the curves $\gamma_1, \gamma_2, \gamma_3$, where*

$$\gamma_1: \quad k = 0, \quad h \geq -\frac{1}{2}, \quad \gamma_2: \quad k = (2h + 1)^2, \quad h \geq -\frac{1}{2}, \quad \gamma_3: \quad k = (2h - 1)^2, \quad h \geq 0,$$

if $\delta = \gamma = 0$. A topological analysis of this case is carried out in [24].

b) *the union of the curves $\Gamma_1, \Gamma_2, \Gamma_3, \Gamma_4, \Gamma_5$, where*

$$\begin{aligned} \Gamma_1: \quad k &= 0, \quad h \geq -\frac{1}{2}, \\ \Gamma_2: \quad k &= 4\gamma^2, \\ \Gamma_3: \quad k &= (2h + 1)^2 + 4\gamma^2, \quad h \geq -\frac{1}{2}, \\ \Gamma_4: \quad k &= (2h - 1)^2, \\ \Gamma_5: \quad k &= \gamma^2(-\gamma^2 + 2 - 4h), \end{aligned}$$

if $\delta = 0$.

c) *the union of the curves $\Delta_1, \Delta_2, \Delta_3, \Delta_4, \Delta_5$, where*

$$\begin{aligned} \Delta_1: \quad k &= 0, \quad h \geq -\frac{1}{2}, \\ \Delta_2: \quad k &= 4\delta^2, \\ \Delta_3: \quad k &= (2h - 1)^2 + 4\delta^2, \\ \Delta_4: \quad k &= (2h + 1)^2, \\ \Delta_5: \quad k &= \delta^2(-\delta^2 + 2 + 4h), \end{aligned}$$

if $\gamma = 0$. Qualitatively different bifurcation diagrams are illustrated in Fig. 7, 8, 9.

d) the union of the curves $\sigma_1, \sigma_2, \sigma_3$, where

$$\begin{aligned}\sigma_1: \quad k &= 0, \quad h \geq \frac{1}{2} \frac{\gamma^2 - \delta^2}{\gamma^2 + \delta^2}, \\ \sigma_2: \quad k &= 4(\delta^2 + \gamma^2), \quad h \geq \min\left\{\frac{1}{2} \cos 2t + \gamma \cos t + \delta \sin t\right\}, \\ \sigma_3: \quad \begin{cases} h(t) = \gamma \delta \frac{\cos 2t}{\sin 2t} + \frac{1}{2} \cos 2t + \frac{1}{2}(\delta^2 - \gamma^2), \\ k(t) = \eta_1^2 + 4\eta_2^2, \end{cases} \quad \text{where} \\ \eta_1 &= -2\gamma \delta \frac{\cos^2 2t}{\sin 2t} + (\gamma^2 - \delta^2) \cos 2t + 2 \cos 2t(\gamma \cos t + \delta \sin t) - 2\gamma \cos t + 2\delta \sin t, \\ \eta_2 &= -\gamma \delta \cos 2t + \frac{1}{2}(\gamma^2 - \delta^2) \sin 2t + \sin 2t(\gamma \cos t + \delta \sin t) - \gamma \sin t - \delta \cos t, \end{aligned}$$

if $\delta^2 + \gamma^2 \neq 0$. The examples of the bifurcation diagrams are demonstrated in Fig. 10, 11.

Theorem 3. In all cases the bifurcation sets $\Sigma(0)$ are parts of surfaces of multiple roots of some polynomials.

We describe the Liouville foliation of the energy surface Q_h^3 in the case $\gamma = 0$. The separating curves cut the plane $\mathbb{R}^2(\delta, h)$ into domains, in which the additional integral F has the Morse–Bott type [4]. These curves are illustrated in Fig. 5. At this figure, for each domain in the plane $\mathbb{R}^2(\delta, h)$ we indicate the pair (Q_h^3, W) , where Q_h^3 is an energy surface and W is a molecule; these pairs are denoted by $(Q_h^3, i_k), k = \overline{1, 13}$. There is a natural correspondence between the domains in Fig. 5 and the intervals on the energy axis in Fig. 7–9. The domain of number i_k corresponds to the energy level $h = a_k$. The complete list of (Q_h^3, W) is represented in Table 1.

We now turn to constructing the bifurcation set for nonzero values of the parameter λ . First we consider the case, when $\delta = \gamma = 0$. To find the bifurcation set we need some simple propositions based on the analysis of right-hand sides of the system (1.2) (see also [24]).

Assertion 1. Any fixed point of the flow $\text{sgrad } H$ lies on the hyperplane $r_1 = 0$ or $r_2 = 0$. Any closed trajectory of the flow $\text{sgrad } H$ intersects the hyperplane $r_1 = 0$ or $r_2 = 0$.

Proof.

We have $\dot{s}_i = 0, \dot{r}_i = 0, i = 1, 2, 3$, at any fixed point of the flow. In particular, the third equation of the system (1.2) gives us $\dot{s}_3 = 2r_1r_2 = 0$, whence $r_1 = 0$ or $r_2 = 0$. We now consider an arbitrary closed trajectory. Since the coordinate s_3 depends on time periodically on this trajectory, there exists an instant of time t_0 such that $\dot{s}_3(t_0) = 0$. Therefore, by virtue of the third equation of the system we have $r_1(t_0) = 0$ or $r_2(t_0) = 0$. ■

Assertion 2. Any Liouville torus intersects the hyperplane $r_1 = 0$ or $r_2 = 0$.

Proof.

We take an arbitrary point on the Liouville torus and issue the trajectory from it. This trajectory is either closed or everywhere dense on the torus. The coordinate s_3 depends on time periodically or almost periodically on this trajectory. Then there exists t_0 such that $\dot{s}_3(t_0) = 0$. Therefore, the trajectory (and, consequently, the Liouville torus) intersects the hyperplane $r_1 = 0$ or $r_2 = 0$. ■

Corollary 1. Singular fibers of the Liouville foliation intersect the hyperplane $r_1 = 0$ or $r_2 = 0$.

Proof.

A singular fiber of the Liouville foliation has a fixed point or a closed trajectory. Therefore, it intersects the hyperplane $r_1 = 0$ or $r_2 = 0$. ■

h	Q_h^3	$W(Q_h^3)$
a_1	\mathbb{S}^3	$A \text{ — } A$
a_2	\mathbb{S}^3	$\begin{array}{c} A \\ A \end{array} \begin{array}{c} \nearrow \\ \searrow \end{array} B \text{ — } A$
a_3	\mathbb{S}^3	$\begin{array}{c} A \\ A \end{array} \begin{array}{c} \nearrow \\ \searrow \end{array} C_2 \begin{array}{c} \nwarrow \\ \swarrow \end{array} A$
a_4	$2\mathbb{S}^3$	$\begin{array}{c} A \\ A \end{array} \begin{array}{c} \nearrow \\ \searrow \end{array} C_2 \begin{array}{c} \nwarrow \\ \swarrow \end{array} \begin{array}{c} A \\ A \end{array} \text{ — } \begin{array}{c} A \\ A \end{array}$
a_5	$\mathbb{S}^1 \times \mathbb{S}^2$	$\begin{array}{c} A \\ A \end{array} \begin{array}{c} \nearrow \\ \searrow \end{array} C_2 \begin{array}{c} \nwarrow \\ \swarrow \end{array} A \begin{array}{c} \nwarrow \\ \swarrow \end{array} C_2 \begin{array}{c} \nwarrow \\ \swarrow \end{array} \begin{array}{c} A \\ A \end{array}$
a_6	$\mathbb{S}^1 \times \mathbb{S}^2$	$\begin{array}{c} A \\ A \end{array} \begin{array}{c} \nearrow \\ \searrow \end{array} C_2 \begin{array}{c} \nwarrow \\ \swarrow \end{array} B \begin{array}{c} \nwarrow \\ \swarrow \end{array} \begin{array}{c} A \\ A \end{array} \begin{array}{c} \nwarrow \\ \swarrow \end{array} \begin{array}{c} A \\ A \end{array}$
a_7	$\mathbb{R}P^3$	$\begin{array}{c} A \\ A \end{array} \text{ — } \begin{array}{c} A^* \\ A^* \end{array} \begin{array}{c} \nearrow \\ \searrow \end{array} P_4 \begin{array}{c} \nwarrow \\ \swarrow \end{array} \begin{array}{c} A \\ A \end{array}$
a_8	$\mathbb{R}P^3$	$\begin{array}{c} A \\ A \end{array} \text{ — } \begin{array}{c} A^* \\ A^* \end{array} \begin{array}{c} \nearrow \\ \searrow \end{array} C_2 \begin{array}{c} \nwarrow \\ \swarrow \end{array} \begin{array}{c} A \\ A \end{array}$
a_9	\mathbb{S}^3	$\begin{array}{c} A \\ A \end{array} \begin{array}{c} \nearrow \\ \searrow \end{array} B \text{ — } B \begin{array}{c} \nwarrow \\ \swarrow \end{array} \begin{array}{c} A \\ A \end{array}$
a_{10}	\mathbb{S}^3	$\begin{array}{c} A \\ A \end{array} \begin{array}{c} \nearrow \\ \searrow \end{array} C_2 \begin{array}{c} \nwarrow \\ \swarrow \end{array} A \begin{array}{c} \nwarrow \\ \swarrow \end{array} B \begin{array}{c} \nwarrow \\ \swarrow \end{array} \begin{array}{c} A \\ A \end{array}$
a_{11}	$\mathbb{S}^1 \times \mathbb{S}^2$	$\begin{array}{c} A \\ A \end{array} \begin{array}{c} \nearrow \\ \searrow \end{array} C_2 \begin{array}{c} \nwarrow \\ \swarrow \end{array} B \begin{array}{c} \nwarrow \\ \swarrow \end{array} \begin{array}{c} A \\ A \end{array} \begin{array}{c} \nwarrow \\ \swarrow \end{array} \begin{array}{c} A \\ A \end{array}$
a_{12}	$\mathbb{R}P^3$	$\begin{array}{c} A \\ A \end{array} \text{ — } \begin{array}{c} A^* \\ A^* \end{array} \begin{array}{c} \nearrow \\ \searrow \end{array} P_4 \begin{array}{c} \nwarrow \\ \swarrow \end{array} \begin{array}{c} A \\ A \end{array}$
a_{13}	$\mathbb{R}P^3$	$\begin{array}{c} A \\ A \end{array} \text{ — } \begin{array}{c} A^* \\ A^* \end{array} \begin{array}{c} \nearrow \\ \searrow \end{array} C_2 \begin{array}{c} \nwarrow \\ \swarrow \end{array} \begin{array}{c} A \\ A \end{array}$

Table 1.

Theorem 4. For $\delta = \gamma = 0$ the bifurcation set $\Sigma(\lambda)$ is the union of curves γ_i , $i = \overline{1, 5}$, where

$$\begin{aligned}
 \gamma_1: & \quad \begin{cases} k = 0, \\ h \geq -\frac{1}{2}, \end{cases} \\
 \gamma_2: & \quad k = -8\lambda^2(2h + 1), \quad h \geq -\frac{1}{2}, \\
 \gamma_3: & \quad k = -8\lambda^2(2h - 1), \quad h \geq \frac{1}{2} - \lambda^2, \quad \text{if } 0 < \lambda \leq \frac{1}{2}; \\
 & \quad h \geq -\lambda^2 - \frac{1}{2} + 2\lambda, \quad \text{if } \frac{1}{2} \leq \lambda \leq 1; \quad h \geq \frac{1}{2}, \quad \text{if } \lambda \geq 1, \\
 \gamma_4: & \quad k = (2h + 1 - 2\lambda^2)^2, \quad h \geq -\frac{1}{2} + \lambda^2, \\
 \gamma_5: & \quad k = (2h - 1 - 2\lambda^2)^2, \quad h \geq \lambda^2.
 \end{aligned}$$

Proof.

We study the singularities of the system of the first integrals f_1 , f_2 , H , and F . To obtain the critical points of the momentum mapping we use the condition

$$\text{rank } J < 4, \quad (4.1)$$

where J is the Jacobi matrix of the mapping $H \times F \times f_1 \times f_2$.

The condition (4.1) is valid if and only if all Δ_{ijkl} are equal to zero. Here Δ_{ijkl} are determinants of the matrices consisting of columns of the Jacobi matrix J of numbers $1 \leq i < j < k < l \leq 6$.

Suppose

$$s_1 = 0. \quad (4.2)$$

Then the system of the equations $\Delta_{ijkl} = 0$ can be reduced to one of the following conditions:

$$s_2(s_3 - \lambda) + r_2r_3 = 0, \quad (4.3)$$

or

$$r_1 = 0, \quad (4.4)$$

$$s_2r_3(1 - s_2^2 - 4\lambda s_3 - 2\lambda s_3 - s_3^2 - \lambda^2) + 4\lambda s_3r_2(s_3 + \lambda) = 0. \quad (4.5)$$

In case (4.3) the corresponding critical values are γ_1 , γ_5 . Note that for $h < -\frac{1}{2}$ the integral manifold $J_{h,k} = \{x \in M^4, H = 2h, F = k\}$ is empty. Suppose that the equalities (4.2), (4.4), (4.5) are valid. Taking into account the area integral, we transform (4.5) to the form

$$(r_2(s_3 + \lambda) - s_2r_3) \cdot (s_2^2 - r_3^2 + 4\lambda s_3) = 0. \quad (4.6)$$

Introduce new variables:

$$p_1 = r_2(s_3 + \lambda) - s_2r_3, \quad q_1 = s_2^2 - r_3^2 + 4\lambda s_3.$$

The values of the first integrals H , F and the equation (4.6) in terms of the variables (p_1, q_1) take the form

$$2p_1^2 - q_1 = 2h + 2\lambda^2 + 1, \quad (4.7)$$

$$q_1^2 = 16\lambda^2h + 8\lambda^2 + k, \quad (4.8)$$

$$p_1 \cdot q_1 = 0. \quad (4.9)$$

If $p_1 = 0$, then we have the segment of the parabola γ_4 ; if $q_1 = 0$, then we have the half-line γ_2 , since the Hamiltonian is bounded from below.

Suppose

$$s_2 = 0. \quad (4.10)$$

The condition (4.1) is valid if and only if

$$s_1(s_3 - \lambda) - r_1r_3 = 0, \quad (4.11)$$

or

$$r_2 = 0, \quad (4.12)$$

$$(r_1(s_3 + \lambda) - s_1r_3) \cdot (s_1^2 + r_3^2 + 4\lambda s_3) = 0. \quad (4.13)$$

■

Under the conditions (4.10), (4.11) the critical values are γ_1 and γ_4 .

Suppose that the equalities (4.10), (4.12), (4.13) are valid and introduce new variables

$$p_2 = r_1(s_3 + \lambda) - s_1r_3, \quad q_2 = s_1^2 + r_3^2 + 4\lambda s_3.$$

Then the values of the first integrals H , F and the equation (4.13) in terms of the variables (p_2, q_2) take the form

$$2p_2^2 - q_2 = 2h + 2\lambda^2 - 1, \quad (4.14)$$

$$q_2^2 = 16\lambda^2 h - 8\lambda^2 + k, \quad (4.15)$$

$$p_2 \cdot q_2 = 0. \quad (4.16)$$

If $p_2 = 0$, then we have the segment of the parabola γ_5 ; and if $q_2 = 0$, then we have the half-line γ_3 , since in this case the solutions are real only for $h \geq \frac{1}{2} - \lambda^2$ if $0 < \lambda \leq \frac{1}{2}$; for $h \geq -\lambda^2 - \frac{1}{2} + 2\lambda$ if $\frac{1}{2} \leq \lambda \leq 1$; and for $h \geq \frac{1}{2}$ if $\lambda \geq 1$.

Suppose

$$r_1 = 0, \quad s_1 \neq 0. \quad (4.17)$$

From the system

$$\begin{cases} (s_3 + \lambda)r_2 - s_2r_3 = p_1, \\ (s_3 + \lambda)r_3 + s_2r_2 = 0, \end{cases} \quad (\text{area integral})$$

we obtain

$$\begin{cases} s_2 = -r_3p_1, \\ s_3 = -\lambda + r_2p_1. \end{cases} \quad (4.18)$$

Note that the case $r_3 = 0$ leads to the general situation, which was studied above for $s_2 = 0$. Therefore, under the condition (4.17) the system $\Delta_{ijkl} = 0$ is equivalent to the following system of equations:

$$\begin{cases} p_1 = -\frac{2\lambda r_2}{r_3^2}, \\ s_1^2 = \frac{4\lambda^2 - r_3^4}{r_3^2}. \end{cases} \quad (4.19)$$

Substituting (4.17), (4.18), (4.19) into the Hamiltonian H and the additional integral F , we obtain the critical values:

$$h = -\frac{1}{2} - \lambda^2 + \frac{4\lambda^2}{r_3^4}, \quad k = -16\lambda^2 \left(\frac{4\lambda^2}{r_3^4} - \lambda^2 - 1 \right).$$

Eliminating the variable r_3 , we come to the familiar relationship between h and k with the same restriction to the value of the energy h . The analysis of the condition $r_2 = 0, s_2 \neq 0$ is carried out analogously.

To complete the proof we use the fact that all singular fibers of the Liouville foliation intersect the hyperplane $r_1 = 0$ or $r_2 = 0$. Theorem is proved.

Corollary 2. *The bifurcation set $\Sigma(\lambda) \setminus \gamma_1$ is a part of surfaces of multiple roots of the polynomials $R_{1,2}(p)$, where*

$$R_{1,2}(p) = (2p^2 - 2h \mp 1 - 2\lambda^2)^2 - 16\lambda^2 h \mp 8\lambda^2 - k.$$

Proof.

We can obtain the polynomials $R_{1,2}(p)$ after eliminating the variable q_1 from the system (4.7), (4.8) and the variable q_2 from the system (4.14), (4.15). By virtue of (4.9), (4.16) the polynomials $R_{1,2}(p)$ have multiple roots. ■

We study the structure of the bifurcation set $\Sigma(\lambda)$. Since $\Sigma(\lambda) = \Sigma(-\lambda)$, we restrict ourselves to the case $\lambda > 0$ (recall that the case $\lambda = 0$ is studied in [24]). The coordinates of the points of intersections of the bifurcation curves are as follows: $\gamma_1 \cap \gamma_{2,3}: (k, h) = (0, \mp \frac{1}{2})$; $\gamma_1 \cap \gamma_{4,5}: (k, h) = (0, \mp \frac{1}{2} + \lambda^2)$; $\gamma_4 \cap \gamma_5: (k, h) = (1, \lambda^2)$. For $0 < \lambda < \frac{1}{2}$ the half-line γ_3 touches the parabola γ_5 at

the point Z_4 , having the coordinates $(k, h) = (16\lambda^4, \frac{1}{2} - \lambda^2)$; and for $\frac{1}{2} < \lambda < 1$ it intersects the parabola γ_4 at the point Z_7 , having the coordinates $(k, h) = (16\lambda^2(\lambda - 1)^2, -\lambda^2 - \frac{1}{2} + 2\lambda)$. The qualitatively different types of the sets (bifurcation diagrams) $\Sigma(\lambda)$ are demonstrated in Fig. 12 a)–c): a) $0 < \lambda < \frac{1}{2}$; b) $\frac{1}{2} < \lambda < 1$; c) $\lambda > 1$. Gathering together all information obtained, we represent the list of the stationary points of the system (1.2) and the corresponding values of the first integrals (which are intersections of the bifurcation curves):

- $r_2 = r_3 = 0, \quad r_1^2 = 1, \quad s_1 = s_2 = s_3 = 0, \quad (k, h) = (0, \frac{1}{2});$
- $r_1 = r_3 = 0, \quad r_2^2 = 1, \quad s_1 = s_2 = s_3 = 0, \quad (k, h) = (0, -\frac{1}{2});$
- $r_1 = r_2 = 0, \quad r_3^2 = 1, \quad s_1 = s_2 = 0, \quad s_3 = -\lambda, \quad (k, h) = (1, \lambda^2);$
- for $\lambda \in (\frac{1}{2}, 1)$: $r_2 = s_2 = 0, \quad r_1^2 = 2\lambda - 1, \quad r_3^2 = 2(1 - \lambda),$
 $s_1 = -\frac{2\lambda r_1 r_3}{1 + r_1^2}, \quad s_3 = -\frac{\lambda(1 - r_1^2)}{1 + r_1^2}, \quad (k, h) = (16\lambda^2(\lambda - 1)^2, -\lambda^2 - \frac{1}{2} + 2\lambda).$

To find number of Liouville tori in each connected component of the domain $\mathbb{R}^3 \setminus \Sigma(\lambda)$ we use methods of computer modelling and the fact that any Liouville torus intersects the hyperplane $r_1 = 0$ or $r_2 = 0$.

On the bifurcation diagram we draw all kinds of “regular” lines $h = a_i$ (and then fix an energy surface Q_h). Changing continuously the value of the additional integral F along these lines, we calculate the Fomenko graphs. Here we use numerical methods to solve the system of differential equations (1.2) and to construct phase trajectories with initial data that are determined for the given triple (λ, k, h) from the following system:

$$\begin{cases} s_{1,2} = r_{1,2} = 0, \\ R_{1,2}(p_{1,2}) = 0, \\ q_{1,2} = 2p_{1,2}^2 - 2h \mp 1 - 2\lambda^2, \\ (1 \mp p_{1,2}^2)r_{2,1}^2 \pm 4\lambda p_{1,2}r_{2,1} - 1 \pm (p_{1,2}^2 - q_{1,2} - 4\lambda^2) = 0, \\ r_3^2 = 1 - r_{2,1}^2, \\ s_{2,1} = -p_{1,2}r_3, s_3 = r_{2,1}p_{1,2} - \lambda, \end{cases} \quad (4.20)$$

where

$$p_{1,2} = r_{2,1}(s_3 + \lambda) - s_{2,1}r_3, \quad q_{1,2} = s_{2,1}^2 \mp r_3^2 + 4\lambda s_3.$$

We actually use the fact that for the polynomials $R_{1,2}(p)$ the bifurcation curves are discriminant. The number of roots of the polynomials (i. e. the number of connected components) may change only after going through the discriminant curve¹. Thus, choosing a point (λ, k, h) in each connected component of the domain $\mathbb{R}^3 \setminus \Sigma(\lambda)$ and issuing the trajectory with the initial data (4.20), we can determine number of tori in each connected component of the domain $\mathbb{R}^3 \setminus \Sigma(\lambda)$. To do this it is sufficient to find how many domains are filled with phase curves everywhere dense. The number of tori is indicated in Fig. 12.

We show that for $0 < \lambda < 1$ the segment Z_2 – Z_5 corresponds to the atom A^* . As it was proved in Theorem 1, for $h < 0$ the manifold Q_h^3 is the union of two spheres \mathbb{S}^3 . Consequently, in particular, on the line $k = 0$ there are two separated bifurcations of a torus to a torus. For $0 < \lambda < 1$ the preimage

¹This is supported by Appelrot [1] and Kharlamov [18] devoted to the Kovalevskaya gyroscope. In the first paper domains of “real motions” (i. e. the projections of the integral manifold onto the equatorial plane) are studied in dependence on number and location of real roots of the basic polynomial. In the second one number of preimages of each interior point of domains of real motions is specified. Then it is possible to find number of Liouville tori, corresponding to any component of the complement to the discriminant of the basic polynomial.

of the segment $k = 0$, $-\frac{1}{2} + \lambda^2 < h < \frac{1}{2}$ is the critical set $s_1 = s_2 = r_3 = 0$, which can be represented in space (r_1, r_2, s_3) as intersection of two surfaces

$$\Gamma_{1,2}: \quad \begin{cases} s_3^2 + r_1^2 = a^2, \\ s_3^2 - r_2^2 = a^2 - 1, \end{cases}$$

where $a = \sqrt{h + \frac{1}{2}}$. On the segment Z_2 – Z_5 we have $\lambda < a < 1$. Putting

$$s_1 = s_2 = r_3 = 0 \quad (4.21)$$

in (1.2), we find the parametric representation of the closed curves $\Gamma_{1,2} \cong \mathbb{S}^1$ in terms of the Jacobi functions with the modulus a

$$\Gamma_{1,2}: \quad \begin{cases} r_1 = \pm a \operatorname{sn} \varphi, \\ r_2 = \pm \operatorname{dn} \varphi, \\ s_3 = -a \operatorname{cn} \varphi, \end{cases} \quad \text{where } \varphi = 2(t - t_0). \quad (4.22)$$

We consider the solution (4.21) and Γ_1 . Through the point $\varphi = 0$ we draw the hyperplane $r_1 = 0$, which is orthogonal to this trajectory. Its intersection with the level $J_{h,0} = \{x \in T^*\mathbb{S}^2: H = 2h, F = 0\}$ is determined by the following equations:

$$\begin{aligned} r_2^2 + r_3^2 &= 1, & s_2 r_2 + (s_3 + \lambda) r_3 &= 0, & s_1^2 + s_2^2 + 2s_3^2 + r_3^2 &= 2a^2, \\ (s_1^2 + s_2^2)^2 + 2r_3^2(s_1^2 - s_2^2) + r_3^4 + 8\lambda(s_3 - \lambda)(s_1^2 + s_2^2) + 8\lambda r_2 r_3 s_2 &= 0. \end{aligned}$$

Taking the value r_3 as a small parameter ε in the neighborhood of the trajectory, we obtain the parametric formulas for the surface $J_{h,0}$:

$$\begin{aligned} r_1 &= 0, & r_2 &= 1 - \frac{\varepsilon^2}{2}, & r_3 &= \varepsilon, \\ s_1 &= \pm \sqrt{\frac{a - \lambda}{a + \lambda}(1 + \lambda^2 - a^2)}, & s_2 &= -\varepsilon(\lambda - a), & s_3 &= -a + \frac{\varepsilon^2}{2(\lambda + a)}, \end{aligned}$$

Clearly, this is the “cross”. Since the bifurcation has the form $\mathbb{T}^2 \rightarrow V \rightarrow \mathbb{T}^2$, this is possible only if $V = A^*$. For the other solution (4.21) and Γ_2 the arguments are the same.

We note that the equations (4.21)–(4.22), like in the Sretensky case [19], can form the basis for study splitting of separatrices [21, 22].

It can be shown that for $0 < \lambda < 1$ the point Z_5 , having the coordinates $(k, h) = (0, \frac{1}{2})$, is a “saddle-saddle” point of zero-rank multiplicity 2 (its preimage contains two nondegenerate points of zero rank). In the neighborhood of this point the bifurcation diagram is homeomorphic to two transversal intervals with a common point. The loop molecule has the form illustrated in Fig. 4. All loop molecules that correspond to the saddle-saddle points of multiplicity 2 are described in [6]. The complete list contains 39 molecules. There are exactly 2 molecules (V_1, V_2) in the list that fit our case: they are (P_4, C_2) and (L_1, D_2) . In any case, as V_3 we have the bifurcation $2B$.

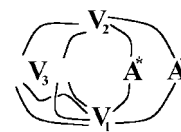


Fig. 4

In order to distinguish the atoms C_2 and D_2 , we use one of the most important property of atoms — the symmetry². It is known that the atom D_2 has no symmetries, interchanging singular one-dimension orbits, whereas the symmetry group of the atom C_2 is $\mathbb{Z}_2 \times \mathbb{Z}_2$ [4]. In our problem we can represent this symmetry group in an explicit form.

²In general, the fact that in integrable problems of rigid body dynamics there are atoms different from A and B is a consequence of symmetries of these problems. Therefore, it would be natural to use these internal symmetries to classify bifurcations.

Singular point	Type of singular point	Loop molecule
Z_1	Nondegenerate singular point of "center-center" type	$A \xrightarrow{0} A \quad A \xrightarrow{0} A$
Z_2	Degenerate singular orbit	$A \xrightarrow{\frac{1}{2}} A^* \xrightarrow{0} A \quad A \xrightarrow{\frac{1}{2}} A^* \xrightarrow{0} A$
Z_3	Nondegenerate singular point of "center-saddle" type	$A \xrightarrow{\infty} C_2 \xrightarrow{\infty} A$ $A \xrightarrow{\infty} C_2 \xrightarrow{\infty} A$
Z_4	Degenerate singular point	
Z_5	Nondegenerate singular point of "saddle-saddle" type	
Z_6	Degenerate singular orbit of elliptic type	
Z_7	Nondegenerate singular point of "center-saddle" type	$A \xrightarrow{\infty} P_4 \xrightarrow{\infty} A$ $A \xrightarrow{\infty} P_4 \xrightarrow{\infty} A$
Z_8	Nondegenerate singular point of "center-center" type	$A \xrightarrow{0} A \quad A \xrightarrow{0} A$
Z_9	Nondegenerate singular point of "center-saddle" type	$A \xrightarrow{\infty} C_2 \xrightarrow{\infty} A$ $A \xrightarrow{\infty} C_2 \xrightarrow{\infty} A$
Z_{10}	Degenerate singular orbit of elliptic type	$A \xrightarrow{0} B \xrightarrow{0} A \quad A \xrightarrow{0} B \xrightarrow{0} A$ $A \xrightarrow{0} B \xrightarrow{0} A \quad A \xrightarrow{0} B \xrightarrow{0} A$

Table 2. Loop molecules of the singular points.

Obviously, the system of the first integrals possesses the following symmetries:

- $\tau_1: (s_1, s_2, s_3, r_1, r_2, r_3) \rightarrow (s_1, s_2, s_3, -r_1, -r_2, -r_3),$
- $\tau_2: (s_1, s_2, s_3, r_1, r_2, r_3) \rightarrow (-s_1, s_2, s_3, -r_1, r_2, r_3),$
- $\tau_3: (s_1, s_2, s_3, r_1, r_2, r_3) \rightarrow (s_1, -s_2, s_3, r_1, -r_2, r_3),$
- $\tau_4: (s_1, s_2, s_3, r_1, r_2, r_3) \rightarrow (-s_1, -s_2, s_3, r_1, r_2, -r_3).$

Since all symmetries preserve the first integrals and the level surfaces, they give rise to symmetries of atoms (to each other or to themselves). Since the preimage of each point from the segment (i) (see Fig. 12) is connected, these are symmetries of the atom V_2 to itself. We show that among these symmetries there are symmetries, changing singular circles.

h	Q_h^3	$W^*(Q_h^3)$
a_1	$2\mathbb{S}^3$	$A \xrightarrow{0} A \quad A \xrightarrow{0} A$
a_2	$2\mathbb{S}^3$	$A \xrightarrow{0} A^* \xrightarrow{0} A \quad A \xrightarrow{0} A^* \xrightarrow{0} A$
a_3	$\mathbb{S}^1 \times \mathbb{S}^2$	$ \begin{array}{c} A \xrightarrow{0} A^* \xrightarrow{0} C_2 \xrightarrow{\infty} A \\ A \xrightarrow{0} A^* \xrightarrow{0} C_2 \xrightarrow{\infty} A \end{array} $
a_4	$\mathbb{S}^1 \times \mathbb{S}^2$	$ \begin{array}{c} A \xrightarrow{0} A^* \xrightarrow{0} P_4 \xrightarrow{\infty} A \\ A \xrightarrow{0} A^* \xrightarrow{0} P_4 \xrightarrow{\infty} A \end{array} $
a_5	$\mathbb{R}P^3$	$ \begin{array}{c} A \xrightarrow{0} C_2 \xrightarrow{0} B \xrightarrow{0} A \\ A \xrightarrow{0} C_2 \xrightarrow{0} B \xrightarrow{0} A \end{array} $
a_6	$\mathbb{R}P^3$	$ \begin{array}{c} A \xrightarrow{0} C_2 \xrightarrow{\frac{1}{2}} A \\ A \xrightarrow{0} C_2 \xrightarrow{\frac{1}{2}} A \end{array} $
b	N^3	$ \begin{array}{c} A \xrightarrow{0} A^* \xrightarrow{0} P_4 \xrightarrow{\infty} A \\ A \xrightarrow{0} A^* \xrightarrow{0} P_4 \xrightarrow{\infty} A \end{array} $
c	$\mathbb{S}^1 \times \mathbb{S}^2$	$ \begin{array}{c} A \xrightarrow{0} C_2 \xrightarrow{\infty} A \\ A \xrightarrow{0} C_2 \xrightarrow{\infty} A \end{array} $
d	$\mathbb{S}^1 \times \mathbb{S}^2$	$ \begin{array}{c} A \xrightarrow{0} C_2 \xrightarrow{0} B \xrightarrow{0} A \\ A \xrightarrow{0} C_2 \xrightarrow{0} B \xrightarrow{0} A \end{array} $

Table 3.

As it was proved, each torus and each closed trajectory in the neighborhood of the point Z_5 intersect the hyperplane $r_1 = 0$. Consider the intersection of singular trajectories in the preimage of an arbitrary point of the segment (i) with this hyperplane. The intersection points have the coordinates $(s_1^\circ, s_2^\circ, s_3^\circ, r_1^\circ, r_2^\circ, r_3^\circ)$, where $s_1^{\circ 2} = \frac{4\lambda^2 - r_3^{\circ 4}}{r_3^{\circ 2}}$, $s_2^\circ = \frac{2\lambda r_2^\circ}{r_3^\circ}$, $s_3^\circ = -\frac{\lambda(2 - r_3^{\circ 2})}{r_3^{\circ 2}}$, $r_1^\circ = 0$, $r_2^{\circ 2} = 1 - r_3^{\circ 2}$.

Here r_3° is a root of one (any) of the equations $h + \frac{1}{2} + \lambda^2 = \frac{4\lambda^4}{r_3^{\circ 4}}$ or $k = -16\lambda^2 \left(\frac{4\lambda^2}{r_3^{\circ 4}} - \lambda^2 - 1 \right)$. Since r_3° can be obtained from the equations up to the sign and there is arbitrariness in choosing of signs of the coordinates s_1° and r_2° , we can conclude that two singular trajectories intersect the surface $r_1 = 0$ at eight points, and each trajectory intersects this surface at four points. To separate points lying on the same trajectory we use computer modelling. We take an arbitrary point $(s_1^\circ, s_2^\circ, s_3^\circ, r_1^\circ, r_2^\circ, r_3^\circ)$, issue a trajectory, and observe change of signs of the coordinates s_1 , r_1 , and r_3 , when the trajectory meets the hyperplane $r_1 = 0$. The results of computer analysis are as follows. The sequential points of intersection of the trajectory with the surface $r_1 = 0$ are

$$(s_1^\circ, s_2^\circ, s_3^\circ, 0, r_2^\circ, r_3^\circ) \rightarrow (s_1^\circ, -s_2^\circ, s_3^\circ, 0, -r_2^\circ, r_3^\circ) \rightarrow (-s_1^\circ, -s_2^\circ, s_3^\circ, 0, r_2^\circ, -r_3^\circ) \rightarrow (-s_1^\circ, s_2^\circ, s_3^\circ, 0, -r_2^\circ, -r_3^\circ).$$

Therefore, we know which four points lie on the chosen trajectory. The remaining four points belong to the second one:

$$(-s_1^\circ, s_2^\circ, s_3^\circ, 0, r_2^\circ, r_3^\circ) \rightarrow (s_1^\circ, s_2^\circ, s_3^\circ, 0, -r_2^\circ, -r_3^\circ) \rightarrow (-s_1^\circ, -s_2^\circ, s_3^\circ, 0, r_2^\circ, -r_3^\circ) \rightarrow (-s_1^\circ, -s_2^\circ, s_3^\circ, 0, -r_2^\circ, r_3^\circ).$$

It remains to choose symmetries τ_i that take the points of intersection of the first trajectory with the hyperplane $r_1 = 0$ to the points of intersection of the second one with the same hyperplane. Obviously, the symmetries obtained interchange the singular trajectories. After examining each symmetry τ_i we obtain that τ_1, τ_2 interchange the trajectories and τ_3, τ_4 do not. Besides, we see that τ_1 and τ_2 generate the entire symmetry group of the atom C_2 . Analogously, we can prove that the atom realized at the segment (j) (see Fig. 12) is P_4 .

Consequently, by the theorem on classification of “saddle-saddle” points of zero-rank multiplicity 2 [6] the loop molecule with the given atoms is unique; it is illustrated in Fig. 2. The information about the remaining singular points Z_1 – Z_{10} and their loop molecules is indicated in Table 2.

If we know bifurcations of Liouville tori in neighborhoods of singular points, then we can calculate the numerical marks r_i of the molecule W^* on the corresponding energy surfaces Q_h^3 for any fixed λ and h . To find the marks r_i we use the method of summing loop molecules [4]. For each domain in the plane $\mathbb{R}^2(\lambda, h)$ Fig. 6 illustrates the pair (Q_h^3, W^*) , which consists of the energy surface Q_h^3 and the marked molecule W^* , but with the marks r_i . In this figure the pairs are denoted by $(Q_h^3, i), i = \overline{1, 9}$. There is natural correspondence between zones in Fig. 6 and energy intervals in Fig. 12 a)–c). The energy levels $h = a_i$ correspond to the zones of numbers $i = 1, 2, 3, 4, 5, 6$, and the energy levels $h = b, c, d$ correspond to the zones of numbers $i = 7, 8, 9$, respectively. The complete list (Q_h^3, W^*) is represented in Table 3.

In conclusion we formulate the theorem for almost general case. It can be proved using the same scheme and will be published in a separate paper.

Theorem 5. *The bifurcation set $\Sigma(\lambda)$ is*

a) *the union of curves $\Delta_i(\lambda)$, where*

$$\begin{aligned} \Delta_1(\lambda) : & \begin{cases} k = 4\delta^2, \\ h \geq -\frac{1}{2} - \delta, \end{cases} \\ \Delta_2(\lambda) : & k = (2h - 1 - 2\lambda^2)^2 + 4\delta^2, \\ \Delta_3(\lambda) : & \begin{cases} k = -16\lambda^2 p^2 + 16\lambda\delta p + 16\lambda^4 - \frac{16\lambda^3\delta}{p} + \frac{4\lambda^2\delta^2}{p^2}, \\ h = -\frac{1}{2} - \lambda^2 + p^2 + \frac{\lambda\delta}{p}, \end{cases} \\ \Delta_4(\lambda) : & k = 4(\delta^2 - 4\lambda^2)h - \delta^4 + 4\lambda^2\delta^2 + 2\delta^2 + 8\lambda^2, \end{aligned}$$

if $\gamma = 0$. The example of a bifurcation diagram is illustrated in Fig. 13.

b) *the union of curves $\Gamma_i(\lambda)$, where*

$$\begin{aligned} \Gamma_1(\lambda) : & \begin{cases} k = 4\gamma^2, \\ h \geq -\frac{1}{2} - \frac{\gamma^2}{4}, \end{cases} \\ \Gamma_2(\lambda) : & k = (2h + 1 - 2\lambda^2)^2 + 4\gamma^2, \\ \Gamma_3(\lambda) : & \begin{cases} k = -16\lambda^2 p^2 + 16\lambda\gamma p + 16\lambda^4 - \frac{16\lambda^3\gamma}{p} + \frac{4\lambda^2\gamma^2}{p^2}, \\ h = \frac{1}{2} - \lambda^2 + p^2 + \frac{\lambda\gamma}{p}, \end{cases} \\ \Gamma_4(\lambda) : & k = -4(\gamma^2 + 4\lambda^2)h - \gamma^4 - 4\lambda^2\gamma^2 + 2\gamma^2 - 8\lambda^2, \end{aligned}$$

if $\delta = 0$. The example of a bifurcation diagram is illustrated in Fig. 14.

It can be shown that the bifurcation sets, like in the previous cases, are parts of surfaces of multiple roots of some polynomials. For each case we find the complete list of the Fomenko invariants. Here the atom P_4 bifurcates to more simple atoms $2B$ and C_2 ; this effect shows that the atom P_4 is unstable under perturbations.

References

- [1] *G. G. Appelrot*. Not completely symmetric heavy gyroscopes. In: Motion of a rigid body about a fixed point. Dedicated to the memory of S. V. Kowalevski. Moscow–Leningrad, 1940, P. 61–155.
- [2] *V. I. Arnold*. Mathematical methods in classical mechanics. New York, Springer, 1989.
- [3] *A. V. Bolsinov*. Methods of calculation of the Fomenko–Zieschang invariant. Adv. in Soviet Math., 1991, V. 6, P. 147–183.
- [4] *A. V. Bolsinov, A. T. Fomenko*. Integrable Hamiltonian systems. Geometry, topology, classification. V. 1,2, Izhevsk, 1999.
- [5] *A. V. Bolsinov, A. T. Fomenko, P. H. Richter*. The method of loop molecules and the topology of the Kovalevskaya top. (to appear)
- [6] *A. V. Bolsinov, V. S. Matveev*. Integrable Hamiltonian Systems: Topological structure of saturated neighborhoods of nondegenerate singular points. In book: Tensor and vector analysis. *A. T. Fomenko, O. V. Manturov, V. V. Trofimov* (eds.). Gordon and Breach Science Publish, Australia–Canada, 1998, P. 31–56.
- [7] *S. A. Chaplygin*. A new particular solution to the problem on motion of a rigid body in fluid. In: Complete works. V. 1. Theoretical Mechanics. Mathematics, Moscow, 1948, P. 337–346.
- [8] *A. I. Dokshevich*. Analytical study of a motion of the Kovalevskaya top in the Delone case. Mekh. Tverdogo Tela, Kiev, 1989, № 21, P. 18–20.
- [9] *A. I. Dokshevich*. Two classes of motion of the Kovalevskaya top. Prikl. Matem. Mekh., 1981, V. 45, № 4, P. 745–749.
- [10] *A. I. Dokshevich*. On a particular solution of the Euler–Poisson system under the Kovalevskaya conditions. Mekh. Tverdogo Tela, Kiev, 1980, № 12, P. 16–19.
- [11] *A. I. Dokshevich*. A particular class of motions of the Kovalevskaya top in the Delone case. Mekh. Tverdogo Tela, Kiev, 1990, № 22, P. 15–19.
- [12] *A. T. Fomenko, H. Zieschang*. Criterion of topological equivalence of integrable Hamiltonian systems with two degrees of freedom. Izv. Akad. Nauk SSSR, Ser. Matem., 1990, V. 54, № 3, P. 546–575.
- [13] *I. N. Gashenenko*. Integral manifolds and topological invariants of a case of motion of a gyrost. Mekh. Tverdogo Tela, 1997, № 27, P. 1–7.
- [14] *A. F. Ipatov*. Motion of the Kovalevskaya gyroscope at the boundary of ultraellipticity. Uchen. Zapiski Petrozavod. Univ., Matem. Nauki., 1970, V. 18, № 2, P. 6–93.
- [15] *P. V. Kharlamov*. A case of integrability of equations of motion of a heavy rigid body in fluid. Prikl. Matem. Mekh., 1955, V. 19, № 2, P. 231–233.
- [16] *P. V. Kharlamov*. Integrable cases in the problem on motion of a heavy rigid body in fluid. Dokl. Akad. Nauk SSSR, 1956, V. 107, № 3, P. 381–383.
- [17] *P. V. Kharlamov*. On motion of a body bounded by a multiply connected surface in fluid. Prikl. Mekh. & Tekhn. Fiz., 1963, № 4, P. 17–29.
- [18] *M. P. Kharlamov*. Bifurcations of common levels of the first integrals in the Kowalevski case. Prikl. Matem. Mekh., 1983, V. 47, № 6, P. 922–930.
- [19] *M. P. Kharlamov*. Topological analysis of integrable problems of dynamics of a rigid body. Leningrad, 1988.
- [20] *M. P. Kharlamov, P. E. Ryabov*. Bifurcations of the first integrals in the Kowalevski–Yehia case. Reg. & Chaot. Dyn., 1997, V. 2, № 2, P. 25–40.
- [21] *V. V. Kozlov*. Methods of qualitative analysis in dynamics of a rigid body. Moscow, 1980.
- [22] *V. V. Kozlov*. Symmetries, topology, and resonances in Hamiltonian mechanics. Izhevsk, 1995.
- [23] *S. Kowalevski*. Sur le problème de la rotation d'un corps solide autour d'un point fixe. Acta Math., 1889, V. 12, P. 177–232.
- [24] *O. E. Orel, P. E. Ryabov*. Bifurcation sets in a problem on motion of a rigid body in fluid and in the generalization of this problem. Reg. & Chaot. Dyn., 1998, V. 3, № 2, P. 82–93.
- [25] *A. A. Oshemkov*. Fomenko invariants for the main integrable cases of the rigid body motion equations. Adv. in Soviet. Math., 1991, V. 6, P. 67–146.
- [26] *V. N. Rubanovsky*. Integrable cases in the problem on motion of a heavy rigid body in fluid. Dokl. Akad. Nauk SSSR, 1968, V. 180, № 3, P. 556–559.
- [27] *S. Smale*. Topology and mechanics. Inventiones Mathematicae. I. 10, 1970, № 4, P. 305–331; II. 11, 1970, № 1, P. 45–64.
- [28] *H. M. Yehia*. New integrable problems in the dynamics of rigid bodies with the Kovalevskaya configuration. I — The case of axisymmetric forces. Mech. Res. Com., 1996, V. 23, № 5, P. 423–427.

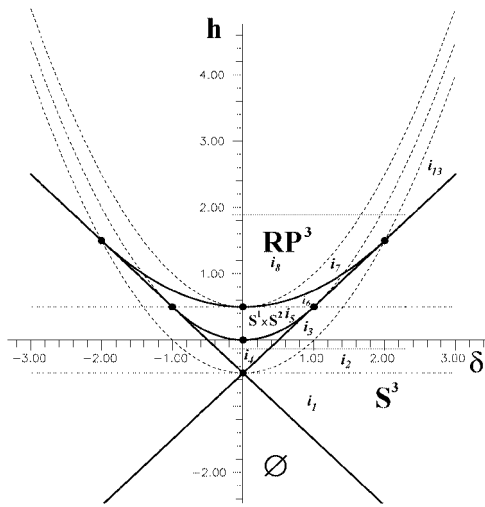


Fig. 5 a)

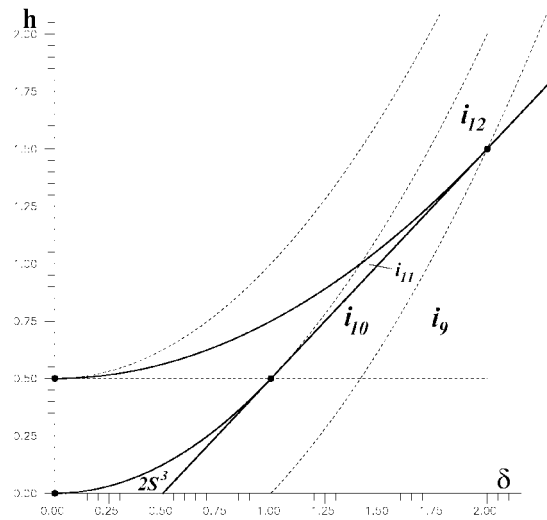


Fig. 5 b)

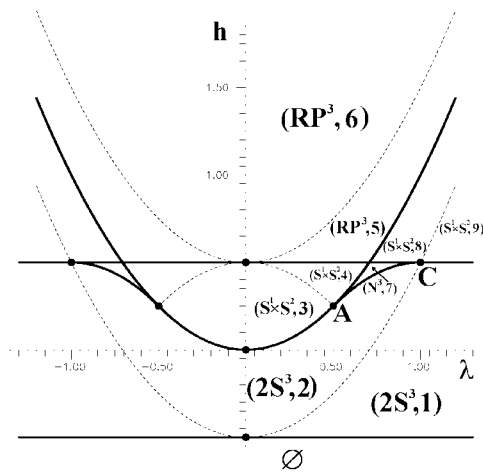


Fig. 6. Topological type of Q_h^3 in the case $\lambda \neq 0, \delta = \gamma = 0$

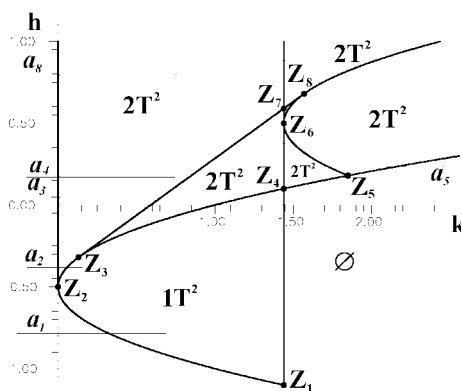


Fig. 7 a)

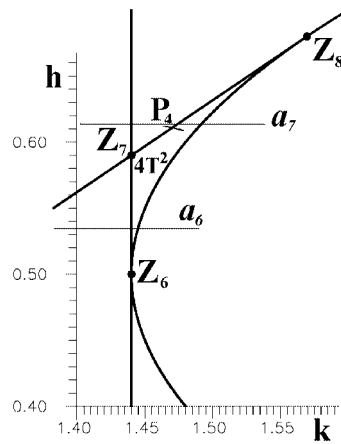


Fig. 7 b)

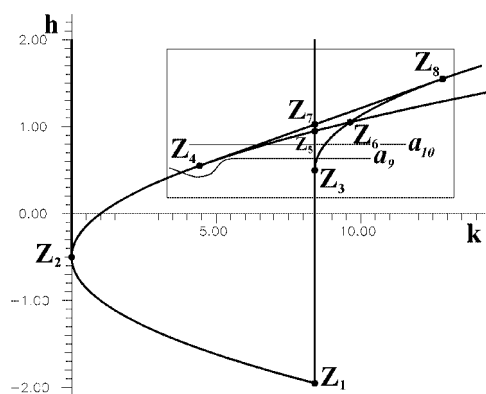


Fig. 8 a)

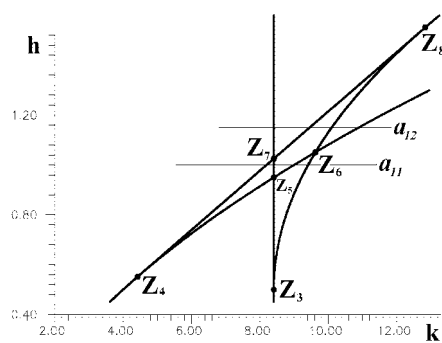


Fig. 8 b)

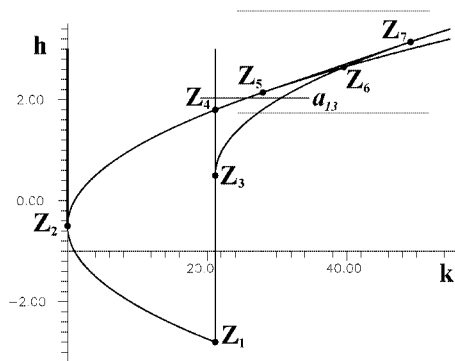


Fig. 9 a)

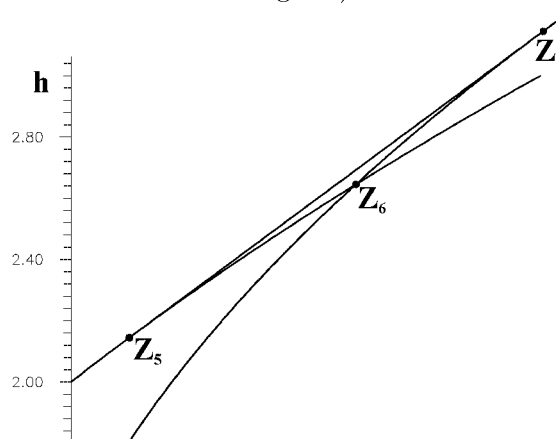


Fig. 9 b)

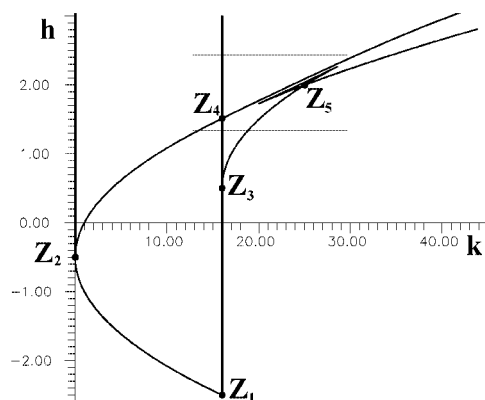


Fig. 10 a)

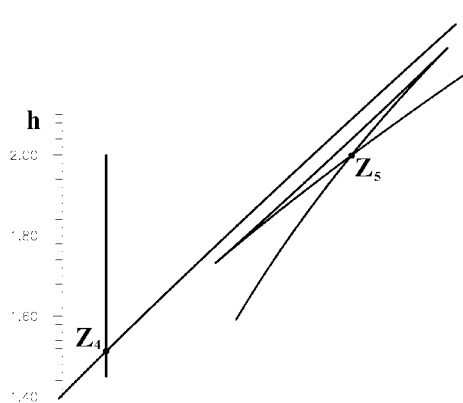


Fig. 10 b)

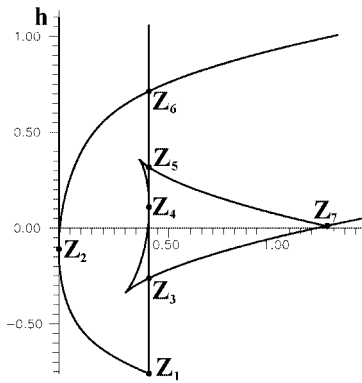


Fig. 11

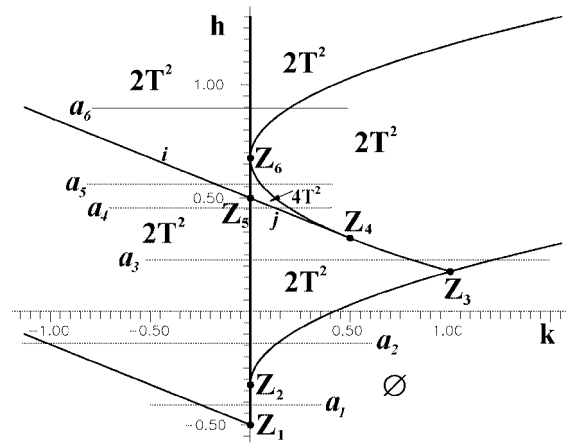


Fig. 12 a) Bifurcation set $\Sigma(\lambda)$ for $0 < \lambda < \frac{1}{2}$

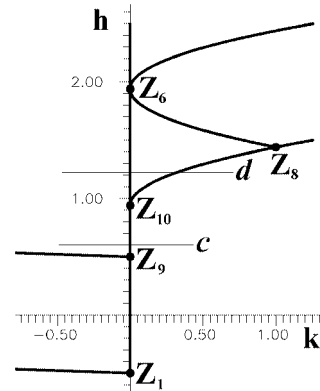
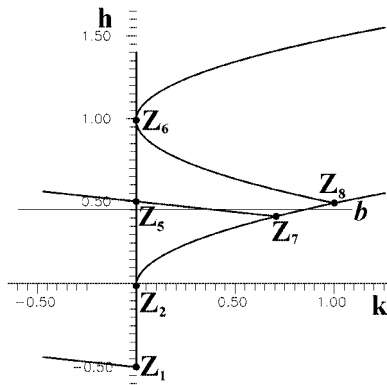


Fig. 12 b) Bifurcation set $\Sigma(\lambda)$ for $\frac{1}{2} < \lambda < 1$ Fig. 12 c) Bifurcation set $\Sigma(\lambda)$ for $\lambda > 1$

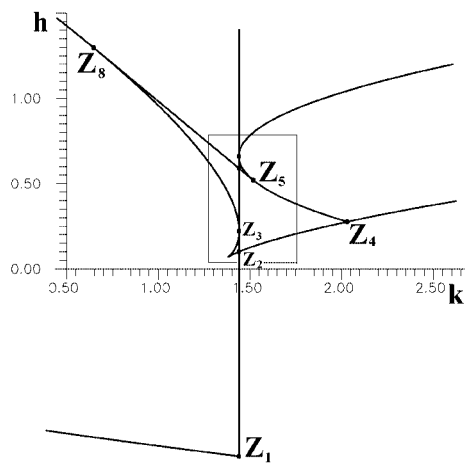


Fig. 13 a)

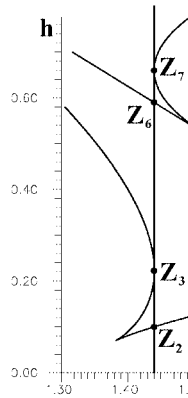


Fig. 13 b)

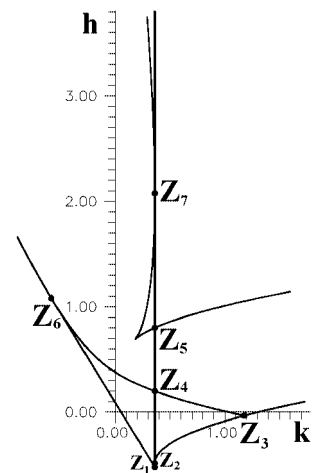


Fig. 14